ELSEVIER

Journal of Photochemistry and Photobiology A: Chemistry 114 (1998) 117–124

Journal of Photochemistry and Photobiology A:Chemistry

Absorption and electrochemical properties of ruthenium(II) dyes, studied by semiempirical quantum chemical calculations

Håkan Rensmo [a], Sten Lunell [b], Hans Siegbahn [c,*]

[a] *Department of Physical Chemistry, University of Uppsala, Box 532, S-75121 Uppsala, Sweden*
[b] *Department of Quantum Chemistry, University of Uppsala, Box 518, S-75121 Uppsala, Sweden*
[c] *Department of Physics, University of Uppsala, Box 530, S-75121 Uppsala, Sweden*

Received 9 December 1997; accepted 14 January 1998

Abstract

The electronic properties of Ru–polypyridine dyes were investigated by means of semiempirical calculations. Intermediate neglect of differential overlap (INDO)/S including configuration interaction (CI) was used to calculate electronic density of state (DOS) structures, transition energies and oscillator strengths. Results for electronic transitions and HOMO energies were compared to absorption spectra and oxidation potentials. The carboxylated form of *cis*-bis(2,2′-bipyridine)bis(isothiocyanato)–ruthenium(II) is an efficient sensitizer in nanostructured photoelectrochemical solar cells. The calculation on this dye reveals a different electronic structure for this complex compared to the other Ru–polypyridine complexes. In this complex, the spatial distribution of the highest occupied molecular orbital is shifted towards the NCS ligands and the electronic transition lowest in energy is assigned to a RuNCS-bpy(π^*) charge transfer transition.

Keywords: Semiempirical quantum chemical calculations; Ruthenium; Ru–polypyridine complex; INDO

1. Introduction

Tris(2,2′-bipyridine)–ruthenium(II) ($Ru(bpy)_3^{2+}$) and its derivatives have attracted considerable attention during the last two decades due to their usefulness as photosensitizers in photoconversion [1,2]. A specific example is the dye sensitization of nanostructured electrodes by carboxylated Ru complexes giving high conversion efficiencies [3–9]. The dye-sensitized photoelectrochemical solar cells differ from the conventional solar cells in that they separate the function of light absorption from the charge carrier transport. In the case of sensitized cells, a photocurrent is generated when a photon, absorbed by a dye molecule, gives rise to an electron injection into the conduction band of the semiconductor particle. The dye is then regenerated by electron transfer from redox species in the solution. Thus, the conversion efficiency depends on energy matching and fast electron transfer between the sensitizing dye and the semiconductor, as well as the dye and the redox species. Insight into the electronic (orbital) structure of these elements is therefore useful in the understanding and optimization of these cells.

In the present paper, we report on the electronic structure and related properties for a variety of Ru complexes [10–12]. The intermediate neglect of differential overlap (INDO) model together with configuration interaction (CI) has been used. Electronic structures and transitions were calculated and the absorption spectra, normally containing charge transfer bands, were reproduced with good accuracy. A comparison between oxidation potentials and calculated HOMO energy levels is included, as well as a closer analysis of the electron structure for some selected complexes. In particular, we focus on the electron structure calculated for *cis*-bis(2,2′-bipyridine)bis(isothiocyanato)–ruthenium(II) ($Ru(bpy)_2(NCS)_2$).

2. Computational method

Electronic structures, transition energies and oscillator strengths were calculated within the INDO/S–CI framework [13–16] using the program package ZINDO [17]. INDO/S–CI is a MO-LCAO-SCF-CI model based on the CNDO and INDO approximations and is parametrized to reproduce

* Corresponding author.

1010-6030/98/$19.00
PII S1010-6030(98)00217-2

spectroscopic properties.[1] To account for electronic relaxation a CI was performed. The CI calculations included a space of the 20 highest occupied and the 10 lowest virtual orbitals involving all single excitations. No geometry optimization was done in the present investigation and the calculations were based on the crystal coordinates.

Complementary ab initio calculations were performed at the 3-21 G(*) level using the program SPARTAN [18].

3. Results and discussion

3.1. General considerations

The energy matching between the dye and the semiconductor is important for efficient energy conversion in a dye-sensitized solar cell. There are several possibilities of changing redox potential and absorption profile of ruthenium dyes [1,2,19]. Effects induced by different ligands on the HOMO and LUMO levels of the complexes are often discussed within the framework of octahedral symmetry using the concept of σ and π donor and acceptor properties of the ligands. Moreover, different ligands have different π^* levels, and since the low energy absorption band is assigned to a metal to ligand charge transfer (MLCT) transition for most Ru–polypyridine complexes, the ligands will affect the absorption profile. The picture retaining the metal and ligand nature of the orbitals within the complex and applying small changes due to ligand–metal interaction is a reasonable first approximation. This is because some of the properties of the ligands and the complexes were found to be correlated (cf. Refs. [20–23]). These correlations give information on how to tune the properties of new complexes. Furthermore, the picture described above is practical in labelling the states involved in redox reactions and electronic transitions.

The INDO/S–CI method on the other hand describes the ground state orbitals as linear combinations of all the valence shell atomic orbitals. In such a delocalized model, the orbitals of the complexes are not primarily analyzed with the use of bonding–backbonding concepts based on σ and π donor and acceptor ability. The interactions between all atoms of the complex were incorporated within the model, normally resulting in a more complex picture. However, for fairly symmetric Ru-complexes, having well-resolved metal and ligand-centred (LC) orbitals, σ and π donor and acceptor properties of the ligands still might be applicable when analyzing the INDO/S–CI results.

3.2. Geometrical considerations

No geometry optimizations are included in the present study. To estimate the importance of geometry, calculations of energy levels and absorption maximum for $Ru(bpy)_3^{2+}$ using different geometries were performed. The Ru–N distance was varied while keeping the geometry within the bipyridyl ligands and the symmetry group (D_3) unchanged.

When changing the Ru–N distance from 2.01 Å to 2.10 Å (the Ru–N distance in $Ru(bpy)_3^{2+}$ is 2.056 Å) the HOMO levels changes from −12.54 eV to −12.65 eV. This difference can be compared with calculations on a series of symmetrical and mixed-ligand, tris chelate complexes of 2,2′-bipyridine, 2,2′-bipyrimidine and 2,2′-bipyrazine. Calculations on these complexes were performed using the geometry of $Ru(bpy)_3^{2+}$ but exchanging the relevant carbons for nitrogens in the ligands. They are included in Table 1 and e.g., for tris(2,2′-bipyrazine)–ruthenium(II), the HOMO level is −13.64 eV. The ligand composition is thus seen to have a larger effect on the HOMO than the changes in Ru–N distance.

A similar conclusion was obtained by calculating the position of the HOMO level in $Ru(bpy)_3^{2+}$ for a Ru–N bond distance of 2.13 Å. This is the Ru–N bonding distance in tris(6,6′-diamino-2,2′-bipyridine)–ruthenium. At this distance the HOMO level for the $Ru(bpy)_3^{2+}$ was calculated to −12.69 eV. This can be compared with −12.18 eV which is the calculated energy for tris(6,6′-diamino-2,2′-bipyridine)–ruthenium(II) using crystal coordinates. The presence of the amino groups thus affects the energy of the HOMO level directly.

The calculated absorption maximum only changes from 430 nm to 404 nm when changing the Ru–N distance from 2.01 Å to 2.10 Å. When comparing this with the different absorption maxima obtained for the complexes in Table 1, the effect of Ru–N bonding distance on the calculated absorption maxima must be considered small.

3.3. Correlations with redox properties

The energy levels involved in redox reactions can be measured by cyclic voltammetry. Measured redox potentials (i.e. free energies) depend on energy changes within the molecule, energy changes depending on the solvent interaction and entropic changes. If the entropic and solvent interaction contributions to the redox potential are fairly similar, as might be assumed for the double charged complexes studied in the present paper, correlations between the experimental oxidation potentials and the calculated HOMO energy levels should be seen. In an earlier work [21], it was shown that the LUMO level of the ligand in Extended Hückel calculations, correlates with the reduction potential for selected Ru complexes. As expected for ruthenium(II)–polypyridine complexes (where the HOMO energy level is expected to be centred on the metal), no correlation was found between the HOMO level of the ligand molecule and the oxidation potential of the complex. Thus, modelling the oxidation potential requires taking both the metal and the ligand into account which may be done within the INDO/S-framework. In Table 1, we summarized our calculations related to the ground state.

[1] For the parameters, the default values set by the program were used ($f_{\sigma\sigma}$ = 1.267 and $f_{\pi\pi}$ = 0.585 and for ruthenium $\beta(5s) = \beta(5p) = -2.0$ and $\beta(4d) = -32.0$).

Table 1
Calculated results listed together with electrochemical and absorption properties

Complex (reference crystal structure)	HOMO (eV)	Oxidation potential (V vs. SCE)[a,c]	ΣE_1[i]	Ru–N bonding distance (Å)	Ru content in HOMO[b]	Experimental absorption spectra[a] ($\varepsilon/10^4$)	Theoretical absorption spectra (ε/a.u.)[f]	M_5[k]
di-carbonyl-bis(2,2′-bipyridyl)–ruthenium [24]	−14.868	>1.9 [25]	3.02	2.088	0.0255	316sh(3.0), 310sh(3.3), 303(3.5), 249(3.6) [26]	315(0.8), 223(1.5)	0.054
tris(3,3′-biisoquinoline)–ruthenium(II) [27]	−11.610	1.12 [28]	1.44	2.070	0.470	386(2.3), 334(9.57) [29]	362sh(1.62), 302(6.19)	0.43
cis-bis(acetonitrile)bis(2,2′-bipyridine)–ruthenium(II) [30]	−12.623	1.44 [25]	1.72	2.047	0.477	426[d] [25]	398(0.28), 263(1.86)	0.50
tris(2,2′-bipyrazine)–ruthenium(II) [31]	−13.559	1.97 [22]	2.16	2.053	0.503	440(1.3), 415sh, 338sh, 291(5.1), 240(2.0) [22]	400(0.385), 299(2.07)	0.49
	−13.642[l]							
(2,2′-bipyridine)-bis(2,2′-bipyrazine)-ruthenium(II)[j]	−13.256	1.71 [22]	1.96					
(2,2′-bipyrazine)-bis(2,2′-bipyridine)–ruthenium(II)[j]	−12.919	1.48 [22]	1.76					
bis(bipyridyl)-(4,5-diazafluoren-9-one)–ruthenium(II) [32]	−12.901	1.36 [33]		2.082	0.555	440(1.41) [33]	411(0.56), 264(2.64)	0.55
tris(1,4,5,8-tetra-azaphenanthrene)–ruthenium(II) [34]	−13.364	1.93 [35]	2.16	2.067	0.441	435(1.6), 407(1.7), 270(3.2) [35]	422sh(0.35), 335sh(1.37), 287(2.17)	0.42
tris(6,6′-diamino-2,2′-bipyridyl)–ruthenium(II) [36]	−12.176	1.05 [37]		2.130	0.516	450(6.3), 380(3.2), 365(3.5), 275(2.5)[e] [37]	435(0.31), 322(1.4), 265(2.12)	0.51
tris(2,2′-bipyridine)–ruthenium(II) [38]	−12.598	1.26 [33]	1.55	2.056	0.526	451(1.3), 285(7.7) [29]	417(0.62), 317(1.01), 262(2.82)	0.53
tris(2,2′-bipyrimidine)–ruthenium(II) [39]	−12.994	1.68 [22]	1.86	2.066	0.537	454(0.86), 418(0.82), 362sh, 332(1.7) [22]	411(0.58), 324(1.36), 235(2.57)	0.54
	−13.031[l]							
(2,2′-bipyridine)-bis(2,2′-bipyrimidine)–ruthenium(II)[j]	−12.873	1.54 [22]	1.76					
(2,2′-bipyrimidine)-bis(2,2′-bipyridine)–ruthenium(II)[j]	−12.735	1.39 [22]	1.66					
cis-bis(2,2′-bipyridine)-bis(pyridine)-ruthenium(II) [40]	−12.577	1.30 [25]	1.53	2.060	0.511	454[d] [25]	495(0.22), 350sh(0.91), 309(1.17)	0.51
bis((2,2′-bipyridine)-isothiocyanato)–ruthenium [41]	−6.7570	0.64 [42]	0.92	2.049	0.258	515(9.3), 360(9.8)[h] [43]	560(0.23), 384(0.47), 275(1.21), 245(1.34)	0.24
cis-di-chloro-bis(2,2′-bipyridine)–ruthenium [44]	6.7364	0.29 [42]	0.57	2.034	0.422	537(9.5), 370(9.5) 300(6.0)[e] [45]	516(0.32), 357(0.54), 274(1.57)	0.49

[a]In acetonitrile.
[b]In dimethylformamide.
[c]In *N*-metylformamide.
[d]In dichloromethane.
[e]In ethanol/methanol (4:1 v/v).
[f]The theoretical absorption maxima and absorption coefficients were taken from calculated spectra, see Fig. 4.
[g]*In the references where also the redox potential for* $Ru(bpy)_3^{2+}$ *is measured, the redox potential for the complex is normalized with respect the redox potential of* $Ru(bpy)_3^{2+}$.
[h]The sum of the squared LCAO coefficients.
[i]The HOMO energy level were calculated using the geometry of $Ru(bpy)_3^{2+}$ (Ru–N bonding distance 2.056 Å).
[j]These values were taken from Ref. [23].
[k]M_5 is the MLCT index including the five transitions lowest in energy ($n=5$) which in most complexes define the absorption peak lowest in energy.

The average (Ru–N) bond length, the experimental oxidation potentials and the summation of the ligand parameters proposed by Lever [23] (ΣE_L) are also included in Table 1.

In particular, the calculated HOMO level is shifted to lower energies in the complex containing carbonyl ligands. Carbonyl ligands were reported to have large π^*-backbonding capacity in ruthenium complexes [26]. In contrast, for the complex containing chloride ligands having π-donor properties [19,45], the calculated HOMO energy level moves to higher energies. The correlation between the HOMO energy level and the oxidation potential for complexes having a charge of 2+ is shown in Fig. 1. It should be noted in considering this correlation that the theoretical calculations only include the intramolecular changes. Therefore, part of the observed deviations can be attributed to differences in solvent interaction. Specifically, uncharged complexes (not shown in Fig. 1) having non-chromophoric ligands are expected to interact with the solvent differently than the charged ones, resulting in changes in the Ru–ligand interaction, i.e., the HOMO levels [45–47].

Most of the calculations were based on crystalline geometries. However, to extend the investigation, calculations on complexes from the work by Rillema et al. [22] were included using the geometry of $Ru(bpy)_3^{2+}$ (see Table 1; the HOMO energies are written in italics). This was done because the crystal coordinates for all the complexes were not available. The redox potentials from these complexes varied from ~1.3 to ~2.0 V vs. SCE and, as seen from Fig. 1 (diamonds), the experimental oxidation potentials correlate very well with the calculated HOMO levels.

Also shown in Fig. 1 is the correlation between the oxidation potential and ΣE_L (see also Ref. [23]). The E_L values were determined empirically by comparing oxidation potentials for different complexes and by assuming that the ligands behave in the same relative way in different metal complexes (ligand additivity). The empirical nature of this method accounts not only for intramolecular changes but also for differences in solvent interactions. As seen in Fig. 1 the ΣE_L values correlate with the oxidation potentials at least as well as the calculated HOMO energies. This is especially true for complexes with different charges (not shown). However, for complexes containing ligands for which the E_L value is unknown the INDO-S method can give valuable information. Moreover, for complexes having extraordinary interaction between the metal and the ligand or between different ligands, the INDO-S method might be preferable.

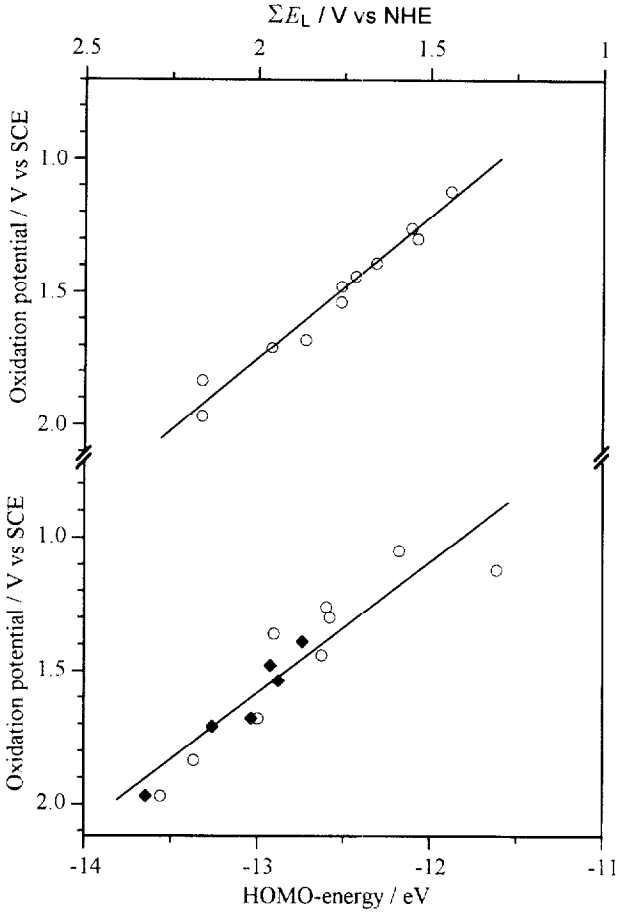

Fig. 1. (a) Correlation between the calculated HOMO levels (lower axis) and oxidation potentials for complexes based on crystal coordinates (circles) and for complexes from the work by Rillema et al. [22] based on the crystal structure of $Ru(bpy)_3^{2+}$ (diamonds). For two complexes, the calculations have been performed using two different structures (the correct crystal structure and the crystal structure of $Ru(bpy)_3^{2+}$, see Table 1). The difference in the HOMO energy for these two complexes can be used to get an estimate of the importance of geometry. (b) Correlation between the ΣE_L (upper axis) and oxidation potential (the E_L values were taken from Ref. [23])

3.4. Density of states

Knowledge of energy level positions is of importance in the study of, e.g., electron transfer processes and chemical reactions. However, insight into the spatial structure of the molecular orbitals obtained by a quantum chemical calculation can also give valuable information. Of particular importance for the present metal complexes is the Ru-content in the HOMO and LUMO levels. For most of the complexes listed in Table 1, the HOMO-orbital contains a large contribution of the Ru atomic orbitals. For example, the HOMO orbital in $Ru(bpy)_3^{2+}$ contains 52% Ru 4d (delocalized π-orbitals contribute with the rest, 44%) and the LUMO orbital is concentrated (99%) on π^*-structure of the ligands (see also Ref. [12]). This structure of the HOMO and LUMO levels is characteristic for most of the complexes studied. Normally, the Ru contribution to the HOMO is around 50% and the contribution to the LUMO is negligible. The results are consistent with a MLCT absorption (or more specifically a $d\pi$ to π^* transition) in the visible region.

Density of states (DOS) spectra for a selected number of complexes are shown in Fig. 2ligand centred (convoluted with Gaussians of FWHM (full width at half maximum) = 0.5 eV). Partial DOS (PDOS) structures are also included to show the contributions of the various building blocks in different regions of the spectra, i.e., it is a representation of the spatial electronic structure. The height of the

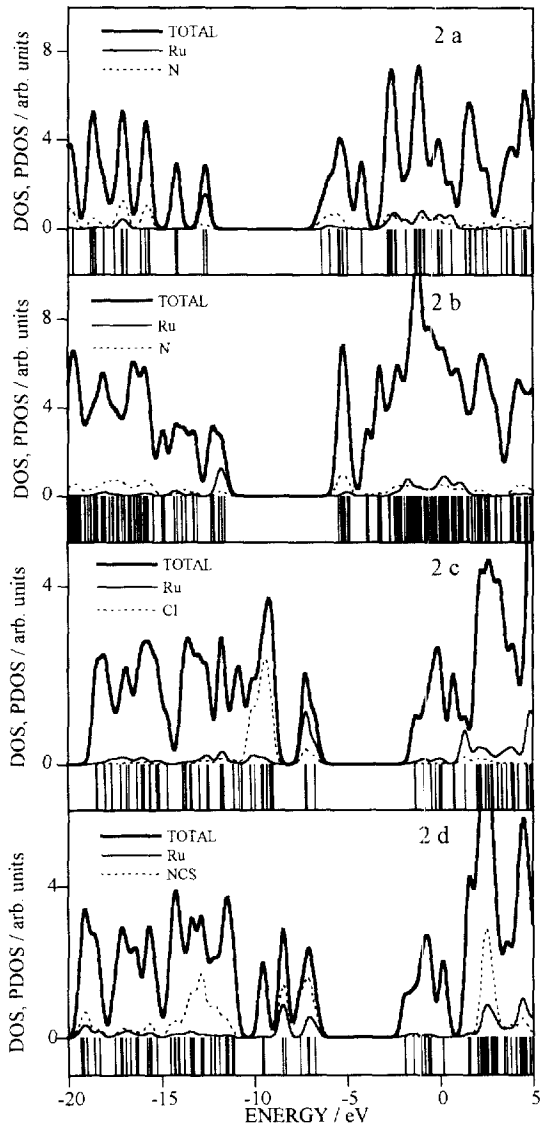

Fig. 2. Calculated DOS and selected PDOS structure for (a) $Ru(bpy)_3^{2+}$, (b) $Ru(i\text{-}biq)_3^{2+}$, (c) $Ru(bpy)_2Cl_2$ and (d) $Ru(bpy)_2(NCS)_2$. The bars represent the calculated energy levels. The DOS and PDOS are calculated by convolution with Gaussians of FWHM = 0.5 eV. The height of these Gaussians is unity when calculating DOS and the sum of the squared LCAO coefficients belonging to an atom or a group of atoms when calculating PDOS.

Gaussians is defined as the sum of the squared LCAO coefficients belonging to an atom or a group of atoms.

For $Ru(bpy)_3^{2+}$, the DOS spectra and PDOS spectra, Fig. 2a, show that the occupied orbitals closest to the energy gap consists of two groups of energy levels. The group at around −13 eV is dominated by the Ru contributions, whereas in the group at −14 eV, such contributions are negligible. For the lowest unoccupied orbitals, the Ru contribution is very small over a broad range.

The ligand contra Ru contributions in the calculated HOMO and LUMO structures are quite similar for tris(3,3′-biisoquinoline)–ruthenium, $Ru(i\text{-}biq)_3^{2+}$. In the DOS-spectrum for $Ru(i\text{-}biq)_3^{2+}$ however, the Ru-dominated HOMO levels are fused into the lower lying ligand dominated orbitals (see Fig. 2b). This affects the absorption spectra such that the visible MLCT transition is shifted almost into the ligand centred (LC) UV transition region (see below). The lowest unoccupied orbitals are again dominated by the ligands.

The HOMO levels in *cis*-di-chloro-bis(2,2′-bipyridine)–ruthenium ($Ru(bpy)_2Cl_2$) are also dominated by Ru. In the DOS-spectrum, Fig. 2c, the Cl contribution is included. As can be seen, the Cl atoms contribute to the HOMO structure. The DOS structure at around −9 eV is mainly due to the Cl atoms. The Cl and Ru contributions in the lowest unoccupied orbitals are almost negligible.

Interestingly, the DOS-spectra suggest a somewhat qualitatively different electronic structure for $Ru(bpy)_2(NCS)_2$ (see Fig. 2d). The two groups of occupied orbitals closest to the energy gap consist almost exclusively of Ru and NCS, and the LUMO structure consists mainly of bipyridine ligands. In the group of occupied orbitals closest to the energy gap, 75% of the NCS PDOS originate from sulphur, i.e., a large part of the HOMO orbitals is shifted towards the sulphur atoms. This shift in weight of the HOMO levels from Ru towards the NCS ligands was reproduced using ab initio calculations (see Fig. 3). For a similar Ru dye, electron spectroscopy experiments also indicate a shift in weight away from the Ru atom [48].

The shift indicates that the positive charge in the oxidized form of $Ru(bpy)_2(NCS)_2$ is shifted towards the NCS ligand. When a Ru dye is used in a solar cell, the excited dye injects electrons into TiO_2 and becomes oxidized. To create a regenerative system, the dye is reduced by redox species (e.g., I^-) in the electrolyte. For a Ru complex containing a NCS ligand [3,6,49], a shift of the HOMO level towards the NCS group may be of importance to facilitate this electron transfer process.

3.5. Absorption properties

An electronic transition implies excitation from the ground state to a Franck–Condon (non-equilibrium) excited state of a molecule. Knowledge of the states involved is of interest for many photoconversion processes. For example, in dye sensitization of semiconductors, not only the absorption maximum and the energy matching between dye and semiconductor is of importance. The type of transition, e.g., LC or MLCT, may also play a vital role.

The calculated results related to the absorption properties of the complexes are included in Table 1 together with the corresponding experimental data. Being obtained from a Hartree–Fock type treatment, the DOS structures for all complexes show an energy gap between the HOMO and LUMO which is overestimated. In order to compare more realistically with the experimental transition energies, a CI among single excitations was performed. As seen from Table 1, the calculated absorption maxima (lowest in energy) thus obtained are in reasonable agreement with experimental data for all complexes. Moreover, the theoretical absorption spectra follow the experimental trends. It should be pointed out that the

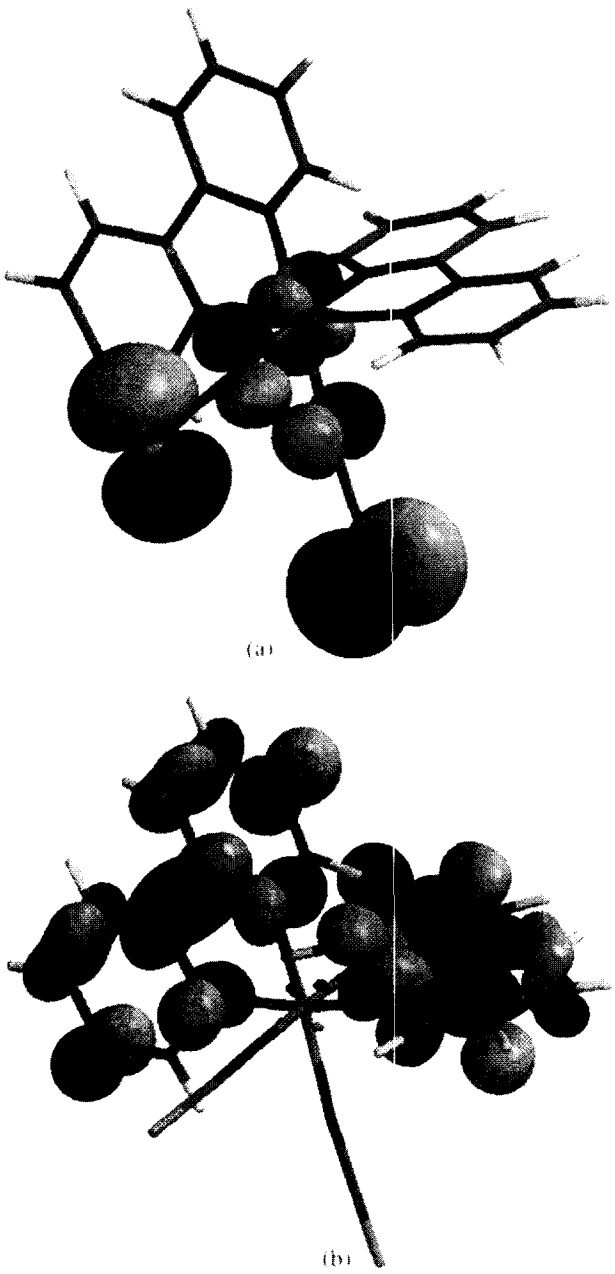

Fig. 3. (a) HOMO and (b) LUMO molecular orbital surfaces for $Ru(bpy)_2(NCS)_2$ calculated at the 3-21 G(*) level using the program SPARTAN. The HOMO and LUMO energies were calculated to be −6.71 eV and −1.90 eV, respectively.

theoretical calculations are made for isolated molecules, thus any interaction with the environment, e.g., solvent interaction, was disregarded [50]. The experimental measurements are made in solution where such interactions may be of importance. This solvent dependence has, however, been found to be very small for $Ru(bpy)_3^{2+}$ [51] and the same can be expected for most of the complexes in Table 1. For complexes containing non-chromophoric charged ligands (e.g., Cl^- or CN^-) the solvent effect has been found to be more important [45,47].

Since the semiempirical calculations are based on linear combinations of all valence atomic orbitals and the calculations include configuration interaction, the description of transitions is more complicated than, e.g., a pure MLCT transitions. Therefore, for the evaluation of the calculated transitions we define the MLCT index, M_n, for a range, n, of transitions.[2] M_n has by definition a value between zero and one. A high value for M_n means that the average electron in the range n of transitions is transferred from orbitals localized mainly at the metal centre (ruthenium atom) in the ground state to orbitals mainly localized on the ligand atoms in the Franck–Condon excited state. A low value means that the MLCT character of the transition is small. It should be emphasized that M_n is an average number used when comparing a number of complexes. Moreover, the selected range, n, affects the index. To get a more complete picture of the transitions, each transition should be analyzed individually.

For $Ru(bpy)_3^{2+}$, the MLCT index including the five transitions lowest in energy (M_5) is calculated to be 0.53. Most of the complexes have a high MLCT index of the same order of magnitude, consistent with a MLCT transition. For some ruthenium(II)carbonyl derivatives (e.g., di-carbonyl-bis(2,2′-bipyridyl)–ruthenium), no well-resolved MLCT bands were observed in the visible region [26]. This is at variance with most of the other polypyridine complexes listed in Table 1. In our calculation, the MLCT index is found to be substantially lower for di-carbonyl-bis(2,2′-bipyridyl)–ruthenium compared to the other complexes. The reason for this is that the Ru orbitals were pushed far into the valence band, resulting in only a minor contribution to the HOMO level (see Table 1). The MLCT band is totally hidden in the LC band at around 315 nm in the calculation.

Theoretical and experimental absorption spectra for a selected number of complexes are shown in Fig. 4. The theoretical spectra were obtained by convolution of Gaussians (height proportional to the oscillator strength and a FWHM of 0.5 eV). The calculated absorption spectra for $Ru(bpy)_2Cl_2$ and $Ru(bpy)_2(NCS)_2$ are shifted towards the red part of the visible region compared to $Ru(bpy)_3^{2+}$ while $Ru(i\text{-}biq)_3^{2-}$ is blue shifted.

The calculated electron transition spectrum for $Ru(bpy)_3^{2+}$ (see Fig. 4a) is satisfactory and similar to the

[2] We define the MLCT index, M_n, as

$$M_n = \frac{1}{\sum_{k=1}^{n} f_k} * \sum_{k=1}^{n} f_k * \sum_{i,j}^{\text{det}} \left(\left(C_{i,j}^{k} \right)^2 * \left(m_{i,j} \right) \right)$$

$$m_{i,j} = \left(\sum_{l}^{\text{Ru}} (c_{i,l})^2 \right) * \left(1 - \left(\sum_{l}^{\text{Ru}} (c_{j,l})^2 \right) \right)$$

In the definition, f_k is the oscillator strength of transition k. C_{ij}^k are the coefficients in the description of transition k, where the subscripts i and j run over all determinants in the space (20 occupied and 10 unoccupied orbitals in the present investigation). In the definition of m_{ij} the coefficient $c_{i,l}$ is the LCAO coefficient of the ground state molecular orbital i. The sums in the definition of m_{ij} run over all Ru d-orbitals. In the present work, the range, n, normally includes the five transitions lowest in energy ($n=5$) which for most complexes define the absorption peak lowest in energy.

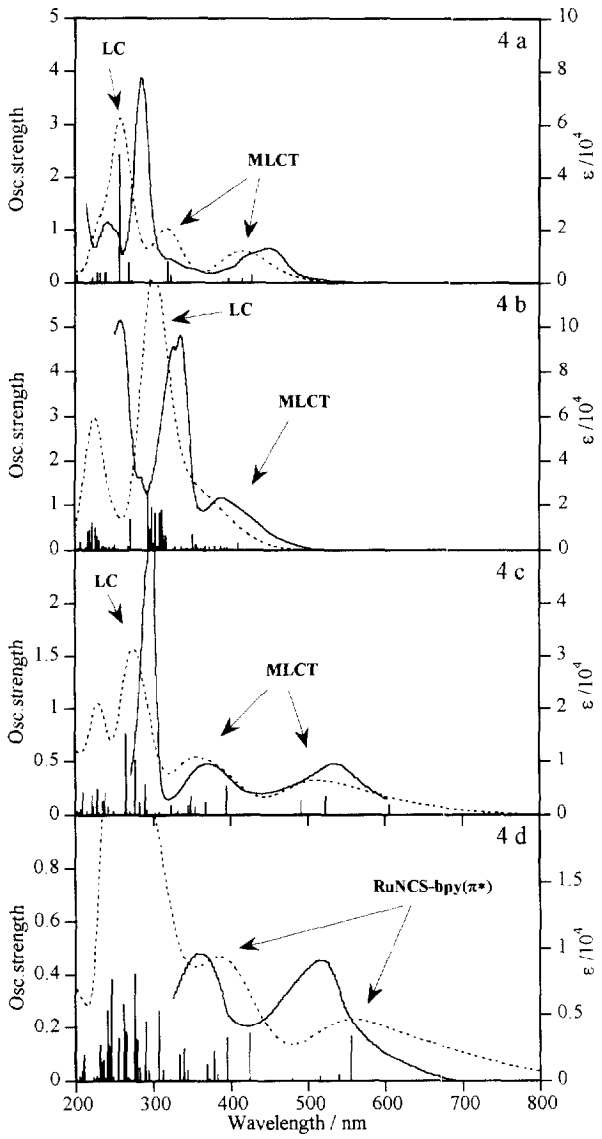

Fig. 4. Calculated absorption spectra (dashed line, left axis) together with experimental absorption spectra (full line, right axis) for (a) $Ru(bpy)_3^{2+}$ in acetonitrile [29], (b) $Ru(i\text{-}biq)_3^{2+}$ in acetonitrile [29], (c) $Ru(bpy)_2Cl_2$ in *N*-methylformamide [45] and (d) $Ru(bpy)_2(NCS)_2$ in dimetylformamide [43]. The absorption spectra are calculated by convolution with Gaussians of FWHM = 0.5 eV and height proportional to the oscillator strength. The bars represent the calculated transitions and oscillator strengths.

earlier reported calculations based on the Extended Hückel approximation [10]. Considering that M_5 is 0.53 and the fact that the contribution from Ru in the levels at around −13 eV and −14 eV (see Fig. 2a) is close to 50 and 0%, respectively, it is concluded that the transitions in the visible region almost exclusively originate from the levels at −13 eV. The structured tail between the intense absorption at around 275 nm and the visible absorption at 450 nm were overestimated in the INDO/S calculation. The present calculations indicate that the transitions in this region have substantial MLCT character. This is in accordance with the calculated results reported by Calzaferri and Rytz [10].

Both the calculated and the experimental absorption spectra are blue shifted for $Ru(i\text{-}biq)_3^{2+}$ compared to $Ru(bpy)_3^{2+}$. In studies of emission spectra $Ru(i\text{-}biq)_3^{2+}$, the emitting state is thought to be of LC type while the lowest absorption energies was assigned to MLCT transitions [29]. In the calculation (see Fig. 4b), we found that the lowest energy absorption for $Ru(i\text{-}biq)_3^{2+}$ is of MLCT type. The conclusion is based on the DOS/PDOS structure and the relatively high MLCT index, $M_5 = 0.43$.

The fact that the $Ru(bpy)_2Cl_2$ is red shifted with respect to $Ru(bpy)_3^{2+}$ is normally explained by the π-donor properties of the Cl^- ions which raise the energy of the occupied Ru-centred orbitals. The red shift is well-reproduced in the INDO/S–CI calculations of $Ru(bpy)_2Cl_2$ (Fig. 4c). However, it is important to remember that the absorption spectra for $Ru(bpy)_2Cl_2$ depend on the solvent; *N*-methylformamide and dimethylformamide give absorption maxima at 538 nm and 568 nm, respectively [45]. In the calculation, the two absorption maxima at 516 nm and 357 nm are built up by five and 10 transitions, respectively. Since $M_5 = 0.47$ and $M_{15} = 0.43$, both maxima are assigned to MLCT transitions.

The carboxylated form of the $Ru(bpy)_2(NCS)_2$ complex has acquired a special interest during recent years due to the fact that it is the most efficient dye so far in nanostructured photoelectrochemical cells [3]. The experimental absorption spectrum for $Ru(bpy)_2(NCS)_2$ together with the calculated one are given in Fig. 4d. Both the experimental and theoretical curves contain two absorption maxima above 300 nm but the theoretical spectra is red shifted. The calculated transition which is lowest in energy, at 672 nm, indicates that the shoulder seen in the experimental spectra originates from an electronically allowed singlet–singlet transition.

Analyzing the theoretical spectra for $Ru(bpy)_2(NCS)_2$ further, the two maxima lowest in energy are built up by five and 10 transitions, respectively. Based on the DOS/PDOS structure and the low MLCT index ($M_5 = 0.24$), we assign the electronic transition lowest in energy to a RuNCS-bpy(π^*) transition, i.e., the NCS group is directly involved in the transition and acts in this sense not just as a spectator ligand. Since $M_{15} = 0.21$, the transition higher in energy, at 384 nm, is also assigned to a RuNCS-bpy(π^*) transition.

4. Conclusion

The electronic structure of selected Ru–polypyridine dyes has been studied using the INDO/S–CI method. The agreement between calculations and experiments in terms of absorption spectra and redox potentials for the complexes was found to be good and the study emphasizes the usefulness of INDO/S–CI to predict electronic properties of Ru–polypyridine dyes.

The result for $Ru(bpy)_2(NCS)_2$ suggests an electronic structure somewhat different from the other complexes studied. The calculated HOMO orbitals for Ru $(bpy)_2(NCS)_2$ are shifted in weight from the Ru atom towards the NCS

ligands. The carboxylated form of this dye, $Ru(CO_2H\text{-}bpy)_2(NCS)_2$, has shown exceptional photoconversion ability in solar cells based on nanostructured materials such as titanium dioxide. The calculated shift in the HOMO level towards the NCS ligand groups is important information for the complete understanding of the role of the dye complex in this type of solar cell.

Acknowledgements

This work was supported by the Swedish Natural Science Research Council (NFR), the Swedish Research Council for Engineering Sciences (TFR) and the Commission of the European Community Joule II and Joule III programs. Martin Agback, Christer Enkvist, Robert Bergström and Petter Persson are gratefully acknowledged for help with the computer programs. We also thank Sven Södergren and Anders Hagfeldt for helpful discussions and Kianosh Lashgari for assistance in finding the proper crystal coordinates.

References

[1] A. Juris, V. Balzani, F. Barigelletti, S. Campagna, P. Belser, A. Von Zelewsky, Coord. Chem. Rev. 84 (1988) 85–277.
[2] K. Kalyanasundaram, Photochemistry of Polypyridine and Porphyrin Complexes, Academic Press, London, 1991.
[3] M.K. Nazeeruddin, A. Kay, I. Rodicio, B.R. Humphry, E. Mueller, P. Liska, N. Vlachopoulos, M. Grätzel, J. Am. Chem. Soc. 115 (1993) 6382–6390.
[4] B. O'Regan, J. Moser, M. Anderson, M. Grätzel, J. Phys. Chem. 94 (1990) 8720–8726.
[5] K. Kalyanasundaram, M.K. Nazeeruddin, M. Grätzel, G. Viscardi, P. Savarino, E. Barni, Inorg. Chim. Acta, 1992, pp. 20–1693.
[6] R. Argazzi, C.A. Bignozzi, T.A. Heimer, F.N. Castellano, G.J. Meyer, Inorg. Chem. 33 (1994) 5741–5749.
[7] A. Hagfeldt, B. Didriksson, T. Palmqvist, H. Lindstroem, S. Södergren, H. Rensmo, S.E. Lindquist, Sol. Energy Mater. Sol. Cells 31 (1994) 481–488.
[8] F. Cao, G. Oskam, P.C. Searson, J. Phys. Chem. 99 (1995) 17071–17073.
[9] R. Knoedler, J. Sopka, F. Harbach, H.W. Guenling, Sol. Energy Mater. Sol. Cells 30 (1993) 277–281.
[10] G. Calzaferri, R. Rytz, J. Phys. Chem. 99 (1995) 12141–12150.
[11] E.C. Constable, C.E. Housecroft, Polyhedron 9 (1990) 1939–1947.
[12] C. Daul, E.J. Baerends, P. Vernooijs, Inorg. Chem. 33 (1994) 3538–3543.
[13] M. Zerner, Reviews in Computational Chemistry, Vol. 2, VCH Publishers, 1991.
[14] M.C. Zerner, G.H. Loew, R.F. Kirchner, U.T. Mueller-Westerhoff, J. Am. Chem. Soc. 102 (1980) 589–599.
[15] J. Ridley, M.C. Zerner, Theor. Chim. Acta 32 (1973) 111–134.
[16] A.D. Bacon, M.C. Zerner, Theor. Chim. Acta 53 (1979) 21–54.
[17] ZINDO Version 1988, The ZINDO program package was developed by M. Zerner and co-workers, Univ. of Florida, Gainesville, Florida.
[18] W.J. Hehre et al., Spartan Ver. 4.0, Wavefunction, Irvine, CA, 1995.
[19] K. Kalyanasundaram, M.K. Nazeeruddin, Chem. Phys. Lett. 193 (1992) 292–297.
[20] E.S. Dodsworth, A.B.P. Lever, Chem. Phys. Lett. 124 (1986) 152–158.
[21] F. Barigelletti, A. Juris, V. Balzani, P. Belser, A. Von Zelewsky, Inorg. Chem. 26 (1987) 4115–4119.
[22] D.P. Rillema, G. Allen, T.J. Meyer, D. Conrad, Inorg. Chem. 22 (1983) 1617–1622.
[23] A.B.P. Lever, Inorg. Chem. 29 (1990) 1271–1285.
[24] H. Tanaka, B.C. Tzeng, H. Nagao, S.M. Peng, K. Tanaka, Inorg. Chem. 32 (1993) 1508–1512.
[25] D.V. Pinnick, B. Durham, Inorg. Chem. 23 (1984) 1440–1445.
[26] J.M. Kelly, C.M. O'Connell, J.G. Vos, J. Chem. Soc., Dalton Trans. 2 (1986) 253–258.
[27] M. Kato, K. Sasano, M. Kimura, S. Yamauchi, Chem. Lett. 10 (1992) 366–7022.
[28] A. Juris, F. Barigelletti, V. Balzani, P. Belser, A. Von Zelewsky, Inorg. Chem. 24 (1985) 202–206.
[29] P. Belser, A. Von Zelewsky, A. Juris, F. Barigelletti, A. Tucci, V. Balzani, Chem. Phys. Lett. 89 (1982) 101–104.
[30] M.J. Heeg, R. Kroener, E. Deutsch, Acta Crystallogr., Sect. C 5 (1985) 684–686.
[31] H. Lai, D.S. Jones, D.C. Schwind, D.P. Rillema, J. Crystallogr. Spectrosc. Res. 20 (1990) 321–325.
[32] L. Zhu, Y. Wang, X. You, Y. Yang, J. Huang, Jiegou Huaxue 11 (1992) 239–243.
[33] V. Balzani, A. Juris, F. Barigelletti, P. Belser, A. Von Zelewsky, Sci. Pap. Inst. Phys. Chem. Res. 78 (1984) 78–85.
[34] C. Piccinni-Leopardi, M. Van Meerssche, J.P. Declercq, G. Germain, Bull. Soc. Chim. Belg. 96 (1987) 79–80.
[35] A. Kirsch-De Mesmaeker, R. Nasielski-Hinkens, D. Maetens, D. Pauwels, J. Nasielski, Inorg. Chem. 23 (1984) 377–379.
[36] K. Araki, M. Fuse, N. Kishii, S. Shiraishi, T. Kodama, Y. Uchida, Bull. Chem. Soc. Jpn. 63 (1990) 1299–1304.
[37] K. Araki, M. Fuse, N. Kishii, S. Shiraishi, Bull. Chem. Soc. Jpn. 65 (1992) 1220–1224.
[38] D.P. Rillema, D.S. Jones, H.A. Levy, J. Chem. Soc., Chem. Commun. 19 (1979) 849–851.
[39] D.P. Rillema, D.S. Jones, C. Woods, H.A. Levy, Inorg. Chem. 31 (1992) 2935–2938.
[40] P.B. Hitchcock, K.R. Seddon, J.E. Turp, Y.Z. Yousif, J.A. Zora, E.C. Constable, O. Wernberg, J. Chem. Soc., Dalton Trans. 7 (1988) 300–9246.
[41] R.H. Herber, G. Nan, J.A. Potenza, H.J. Schugar, A. Bino, Inorg. Chem. 28 (1989) 938–942.
[42] B. Durham, J.L. Walsh, C.L. Carter, T.J. Meyer, Inorg. Chem. 19 (1980) 860–865.
[43] P.E. Hoggard, G.B. Porter, J. Am. Chem. Soc. 100 (1978) 1457–1463.
[44] D.S. Eggleston, K.A. Goldsby, D.J. Hodgson, T.J. Meyer, Inorg. Chem. 24 (1985) 4573–4580.
[45] P. Belser, A. Von Zelewsky, A. Juris, F. Barigelleti, V. Balzani, Gazz. Chim. Ital. 113 (1983) 731–735.
[46] C.J. Timpson, C.A. Bignozzi, B.P. Sullivan, E.M. Kober, T.J. Meyer, J. Phys. Chem. 100 (1996) 2915–2925.
[47] N. Kitamura, M. Sato, H.B. Kim, R. Obata, S. Tazuke, Inorg. Chem. 27 (1988) 651–658.
[48] H. Rensmo, S. Södergren, L. Patthey, K. Westermark, L. Vayssieres, O. Kohle, P.A. Brühwiler, A. Hagfeldt, H. Siegbahn, Chem. Phys. Lett. 274 (1997) 51–57.
[49] O. Kohle, S. Ruile, M. Grätzel, Inorg. Chem. 35 (1996) 4779–4787.
[50] K.K. Stavrev, M.C. Zerner, T.J. Meyer, J. Am. Chem. Soc. 117 (1995) 8684–8685.
[51] E.M. Kober, B.P. Sullivan, T.J. Meyer, Inorg. Chem. 23 (1984) 2098–2104.